Physics Letters A 379 (2015) 1654–1660

Contents lists available at ScienceDirect

Physics Letters A

www.elsevier.com/locate/pla

Persistent currents in metallic rings containing a quantum dot

Lukasz Machura [a,b], Jerzy Łuczka [a,b,*]

[a] Institute of Physics, University of Silesia, Katowice, Poland
[b] Silesian Center for Education and Interdisciplinary Research, University of Silesia, 41-500 Chorzów, Poland

ARTICLE INFO

Article history:
Received 8 April 2015
Received in revised form 23 April 2015
Accepted 24 April 2015
Available online 28 April 2015
Communicated by V.M. Agranovich

Keywords:
Mesoscopic systems
Persistent currents
Quantum dots
Electronic transport
Nanoscale materials

ABSTRACT

Currents in metallic rings with a quantum dot are studied in the framework of a Langevin equation for a magnetic flux passing through the ring. Two scenarios are considered: one in which thermal fluctuations of the dissipative part of the current are modeled by classical Johnson–Nyquist noise and one in which quantum character of thermal fluctuations is taken into account in terms of a quantum Smoluchowski equation. The impact of the amplitude and phase of the transmission coefficient of the electron through a quantum dot on current characteristics is analyzed. In tailored parameter regimes, both scenarios can exhibit the transition from para- to diamagnetic response of the current versus external magnetic flux. The type of response is more robust to changes of the amplitude of the transmission coefficient and more sensitive to changes of the phase around some values.

1. Introduction

In the early 90s after the successful reduction of the signal-to-noise ratio the three groups conducted pioneering experiments with the mesoscopic metallic rings. The careful measurements of Cooper [1], Gold [2], and Gallium–Aluminum–Arsenide/Gallium–Arsenide [3] normal rings have shown the evidence of the existence of the persistent equilibrium currents flowing in the *small metallic pieces of the rotational symmetry* reaffirming an old idea of Friedrich Hund [4]. This very idea concerns the charge transport in normal metallic ring. From the Ohm law we can expect that from the macroscopic point of view such current will die out within the relaxation time for a given material, which for metal is known to be rather short and of the order of 10^{-14} s. However, for sufficiently small circumferences the macroscopic description is no longer valid and ring reaches the region where both macro- and micro-world meet making the requirement for the mesoscopic description [5] of the dynamics. At low enough temperature the effects of quantum coherence of electrons appear. Under the right circumstances some electrons in the ring are able to preserve its coherence which in turn results in a persistent (dissipationless) equilibrium current induced by the static magnetic field. In 1965 Bloch [6] and five years later Kulik [7] confirmed Hund's theory using the quantum-mechanical description. The real interest in the topic of the persistent currents in normal rings arose after 1983 paper by Büttiker et al. [8] where the existence of the persistent currents was shown also in the presence of the elastic dispersions.

First measurements of currents in the diffusive regime [2] have shown rather strong disagreement (10–200 times larger currents amplitudes) with the theoretically anticipated values. Later attempts reduced this dissimilarity to a factor of around 2–3 [9]. Experiments with semiconducting materials in the close to ballistic regime usually agreed with the theory [3,10]. Only recently the scanning SQUID technique was used to record not only the response signal of the rings itself but also from the background. This method gave the possibility of the high precision measurements of the current flowing in 33 different separate Gold rings [11] and finally confirmed qualitatively as well as quantitatively all aspect of the existing theoretical descriptions [12]. The alternative method was used to measure the currents in the Aluminum rings which were deposited on a cantilever [13]. A torque magnetometer whose vibration frequency can be precisely monitored was used as a detector. The measurements were performed with several different cantilevers decorated with a single aluminum ring or arrays of hundreds or thousands of identical Aluminum rings. The analysis of the different magnetic susceptibilities seen in [11,13] based on the two-fluid model was addressed in [14–16].

In this work we present the analysis of electrical currents in the mesoscopic metallic (non-superconducting) ring with the quantum dot. The experiment with the measurements of the phase of the transmission coefficient through a quantum dot in the Coulomb regime was performed in 1995 [17]. Many different aspect of the persistent currents in the same scenario was studied rather inten-

* Corresponding author at: Institute of Physics, University of Silesia, Katowice, Poland. Tel.: +48 32 359 1173; fax: +48 32 258 3653.
E-mail address: jerzy.luczka@us.edu.pl (J. Łuczka).

http://dx.doi.org/10.1016/j.physleta.2015.04.039
0375-9601/

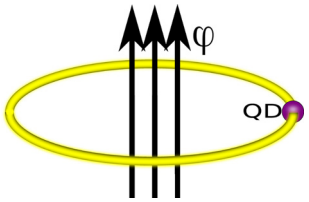

Fig. 1. Schematic picture of the mesoscopic non-superconducting ring with a quantum dot QD. The ring is threaded by a magnetic flux ϕ.

sively over the last two decades [18–22]. Similar schemes with the mesoscopic ring coupled to the quantum dot [23–25] or the quantum ring surrounding the quantum dot – a dot-ring nanostructure (DRN) [26–28] was also addressed. Here we follow the model proposed by Moskalets [29] for a mesoscopic ring containing a potential barrier with a resonant level.

The work is organized in the following way: In Section 2, the model is described and the Langevin equation for the magnetic flux is presented both in the classical and quantum Smoluchowski regimes. Discussion of the results is presented in Section 3. In Section 3.1, the stationary probability distribution of the magnetic flux is analyzed. In Section 3.2, the impact of parameters of the quantum dot on average stationary currents is studied and regimes of paramagnetic and diamagnetic response are worked out. Section 4 contains summary and conclusions.

2. Flux dynamics of mesoscopic metallic rings with a quantum dot

We consider a mesoscopic metallic ring in an external magnetic field B_e applied perpendicular to the plane of the ring (Fig. 1). At zero temperature the ring can display a persistent current I_P when the size of the ring is reduced to the scale of the electron quantum phase coherence length and the thermal length. At non-zero temperature $T > 0$, a part of electrons loses phase coherence due to thermal fluctuations and this part of electrons contributes to a dissipative Ohmic current I_R associated with the resistance R of the metallic ring. The total magnetic flux ϕ piercing the ring is a sum of the external flux $\phi_e \propto B_e$ and the flux due to the flow of the current I, namely,

$$\phi = \phi_e + LI. \tag{1}$$

Here, L stands for the self-inductance of the ring. The current I is a sum of the persistent and dissipative currents,

$$I = I_P + I_R. \tag{2}$$

Now, following Ref. [29], we assume that the ring contains a potential barrier with a resonant level (a quantum dot). The expression for the persistent current $I_P = I_P(\phi)$ in such a system takes the form [29]

$$I_P = I_0\, G(\phi/\phi_0) \sum_{n=1}^{\infty} A_n(T/T^*) \cos[n(k_F l + \bar{\delta}_F)] \times \sin\{n \arccos[t_F \cos(2\pi\phi/\phi_0)]\}, \tag{3}$$

where I_0 is the maximal persistent current at zero temperature for the ring without the quantum dot. The amplitudes $A_n(T/T^*)$ are determined by the relation

$$A_n(T/T^*) = \frac{T/T^*}{\sinh(nT/T^*)}. \tag{4}$$

The characteristic temperature T^* is determined by the energy $k_B T^* = \Delta_F/(2\pi^2)$, where k_B is the Boltzmann constant and Δ_F is the level spacing at the Fermi surface for zero magnetic flux. The magnetic flux ϕ is quantized with the flux quantum $\phi_0 = h/e$ being the ratio of the Planck constant h and the electron charge e. Moreover, k_F is the Fermi momentum and l is the circumference of the ring. The function

$$G(\phi/\phi_0) = \frac{t_F \sin(2\pi\phi/\phi_0)}{\sqrt{1 - t_F^2 \cos^2(2\pi\phi/\phi_0)}} \tag{5}$$

modifies the maximal current due to the quantum dot. Here, t_F and $\bar{\delta}_F$ are the amplitude and phase of the transmission coefficient $T_k = t_k \exp[i\bar{\delta}_k]$ through a quantum dot for an electron with the Fermi momentum $k = k_F$. For $t_F = 1$ and $\bar{\delta}_F = 0$ the expression (3) reduces to a current for a pure metallic ring [30].

According to Ohm's law and Lenz's rule, the dissipative current $I_R = I_R(\phi)$ assumes the form

$$I_R = -\frac{1}{R}\frac{d\phi}{dt} + \sqrt{\frac{2k_B T}{R}}\,\Gamma(t). \tag{6}$$

It means that we include the effect of a nonzero temperature $T > 0$ by adding Johnson–Nyquist noise $\Gamma(t)$ which represents thermal fluctuations. They are modeled by δ-correlated Gaussian white noise of zero mean and unit intensity,

$$\langle \Gamma(t) \rangle = 0, \quad \langle \Gamma(t)\Gamma(s) \rangle = \delta(t-s). \tag{7}$$

Inserting Eqs. (6) and (3) to the relation (1) yields

$$\frac{1}{R}\frac{d\phi}{dt} = -\frac{1}{L}(\phi - \phi_e) + I_P(\phi) + \sqrt{\frac{2k_B T}{R}}\,\Gamma(t). \tag{8}$$

We note that this equation is a Langevin equation for the magnetic flux $\phi = \phi(t)$. Indeed, it has the same form as a Langevin equation for an overdamped motion of a classical Brownian particle subject to the force $F = F(\phi)$ which reads

$$F(\phi) = -\frac{1}{L}(\phi - \phi_e) + I_P(\phi) \tag{9}$$

and the noise intensity strength $D = k_B T/R$ is in accordance with the classical fluctuation–dissipation theorem [31,32]. Therefore we can apply the well-known mathematical and numerical methods for analysis of Eq. (8). First, we transform it to the dimensionless form (see [33,34] for details)

$$\frac{dx}{ds} = -\frac{dV(x)}{dx} + \sqrt{2D_0}\,\xi(s), \tag{10}$$

where $x = \phi/\phi_0$ is the dimensionless magnetic flux. The new time $s = t/\tau_0$, where the characteristic time $\tau_0 = L/R$. The thermal noise intensity $D_0 = k_B T/(\phi_0^2/L) = (E_{T^*}/E_\phi)T_0 = k_0 T_0$, where the dimensionless temperature $T_0 = T/T^*$, $E_{T^*} = k_B T^*/2$ is energy of thermal fluctuations at the characteristic temperature T^*, $E_\phi = \phi_0^2/2L$ is the elementary magnetic energy and $k_0 = E_{T^*}/E_\phi$ rescales intensity of thermal noise. Rescaled Gaussian white noise $\xi(s)$ has exactly the same statistical properties as the dimensional version $\Gamma(t)$. The rescaled potential $V(x)$ takes the form

$$V(x) = \frac{1}{2}(x - x_e)^2 + \alpha W(x). \tag{11}$$

The rescaled external magnetic flux is denoted by $x_e = \phi_e/\phi_0$ and the nonlinearity parameter $\alpha = LI_0/2\pi\phi_0$. The potential consists of the harmonic part $(x - x_e)^2/2$ and the periodic part

$$W(x) = \sum_{n=1}^{\infty} \frac{A_n(T_0)}{n} \cos(n\delta_F) \times \cos\{n \arccos[t_F \cos(2\pi x)]\}, \tag{12}$$

where $\delta_F = k_F l + \bar{\delta}_F$ is a shifted phase.

The Fokker–Planck equation corresponding to the Langevin equation (10) has the form [35]

$$\frac{\partial}{\partial t}P(x,t)=\frac{\partial}{\partial x}\left[\frac{dV(x)}{dx}P(x,t)\right]+D_0\frac{\partial^2}{\partial x^2}P(x,t), \tag{13}$$

where $P(x,t)$ is a probability density of the process determined by Eq. (10). From this equation, all statistical properties of the magnetic flux can be obtained. In particular, its statistical moments $\langle x^k(t)\rangle$ are determined by the expression

$$\langle x^k(t)\rangle=\int_{-\infty}^{\infty}x^k\,P(x,t)dx,\quad k=1,2,3,\ldots \tag{14}$$

For experimentalists, more interesting is the electrical current flowing in the ring. From Eq. (1) it follows that at any time the total current reads

$$I(t)=\frac{1}{L}(\phi(t)-\phi_e) \tag{15}$$

and its average value is given by the relation

$$i(t)=\langle x(t)\rangle-x_e,\quad i(t)=\frac{L}{\phi_0}\langle I(t)\rangle, \tag{16}$$

where the dimensionless current $i(t)$ has been introduced. In the stationary state,

$$i=\langle x\rangle-x_e,\quad \langle x\rangle=\int_{-\infty}^{\infty}x\,P(x)dx, \tag{17}$$

where $P(x)=\lim_{t\to\infty}P(x,t)$ is a stationary probability density. It can easily be calculated from Eq. (13) for $\partial P(x,t)/\partial t=0$ and zero stationary probability current yielding the distribution

$$P(x)=\lim_{t\to\infty}P(x,t)=N_0\exp\left[-\Psi_C(x)\right] \tag{18}$$

and N_0 is the normalization constant. The generalized thermodynamic potential $\Psi_C(x)=V(x)/D_0$ depends on the external flux x_e and the stationary probability density is given by the Boltzmann distribution. Eqs. (17)–(18) form a closed set from which the non-linear function $i=f(x_e)$ can be calculated determining the stationary current-flux characteristics.

2.1. Quantum Smoluchowski limit

Thermal fluctuations modeled as classical δ-correlated white noise are adequate to describe many physical phenomena even in low temperatures. However, in some low temperature regimes, quantum effects like tunneling, quantum reflections and purely quantum fluctuations are playing an increasingly important role and quantum character of thermal fluctuations should be taken into account. How to do it is not a simple task and the problem in a general case is still unsolved. In the so-called quantum Smoluchowski limit, the leading quantum corrections are incorporated in the modified diffusion coefficient D_0 [36–44]. The modified diffusion coefficient takes the form [37]

$$D_\lambda(x)=\frac{1}{\beta(1-\lambda\beta V''(x))},\quad \beta^{-1}=D_0. \tag{19}$$

The prime denotes the differentiation with respect to x. The dimensionless quantum correction parameter

$$\lambda=\lambda_0\left[\gamma+\Psi\left(1+\frac{\epsilon}{T_0}\right)\right], \tag{20}$$

where

$$\lambda_0=\frac{\hbar R}{\pi\phi_0},\quad \epsilon=\frac{\hbar}{2\pi CR}\frac{1}{k_BT^*}. \tag{21}$$

The psi function Ψ is the digamma function (the logarithmic derivative of the gamma function). The $\gamma\approx 0.577$ is the Euler constant and C is capacitance of the system related to the charging effects. The quantum correction parameter λ is a difference between the quantum $\langle x^2\rangle_q$ and classical $\langle x^2\rangle_c$ second statistical moments of the magnetic flux (see Eq. (5) in Ref. [36]),

$$\lambda=\langle x^2\rangle_q-\langle x^2\rangle_c. \tag{22}$$

The modification of the diffusion coefficient (19) results in modification of the Langevin equation, namely,

$$\frac{dx}{ds}=-\frac{dV(x)}{dx}+\sqrt{2D_\lambda(x)}\,\xi(s) \tag{23}$$

and should be interpreted in the Ito sense [35]. The corresponding Fokker–Planck equation has the form

$$\frac{\partial}{\partial t}P(x,t)=\frac{\partial}{\partial x}\left[\frac{dV(x)}{dx}P(x,t)\right]+\frac{\partial^2}{\partial x^2}\left[D_\lambda(x)P(x,t)\right]. \tag{24}$$

The stationary solution of this equation reads

$$P(x)=N_0D_\lambda^{-1}(x)\exp[-\Psi_\lambda(x)], \tag{25}$$

where the generalized thermodynamic potential takes the form

$$\Psi_\lambda(x)=\beta V(x)-\frac{\lambda\beta^2}{2}[V'(x)]^2. \tag{26}$$

We emphasize that the stationary distribution describes an equilibrium state, but it is not a Gibbs state. Remember that the Gibbs state is correct in the limit of a weak coupling of the system with thermostat. The Smoluchowski limit corresponds to the strong coupling regime.

3. Discussion of results

For the ring without a quantum dot, our model reproduces experimental data both for the diamagnetic and paramagnetic response in the vicinity of zero magnetic field [15]. For the ring with a quantum dot, we have not found experimental data. Therefore, our work could inspire experimentalists to design experiments and verify our theoretical predictions revealed below: the influence of the transmission coefficient t_F and the phase δ_F of the quantum dot on stationary current-flux characteristics.

The system has an 8-dimensional parameter space $\{x_e, T_0, k_0, \alpha, \lambda_0, \epsilon, t_F, \delta_F\}$. It would be difficult to carry out a comprehensive analysis and present current-flux characteristics for all possible sets of parameters. Therefore, for numerical calculations, values of the parameters $\alpha=0.1$, $k_0=1$ and $T_0=0.2$ are kept fix. We include quantum corrections which are characterized by 2 parameters: λ_0 and ϵ. Their physical meaning is explained in Refs. [33,34]. Here, they will be fixed at the value of $\lambda_0=0.001$ and $\epsilon=100$. The quantum dot is also characterized by 2 parameters: t_F and δ_F and their impact is displayed below. The similar analysis but for the pure metallic ring without the quantum dot is presented in our previous papers. The stationary solutions of the Fokker–Planck equation was addressed in Ref. [34] and the current-flux characteristics was investigated in Refs. [15,16].

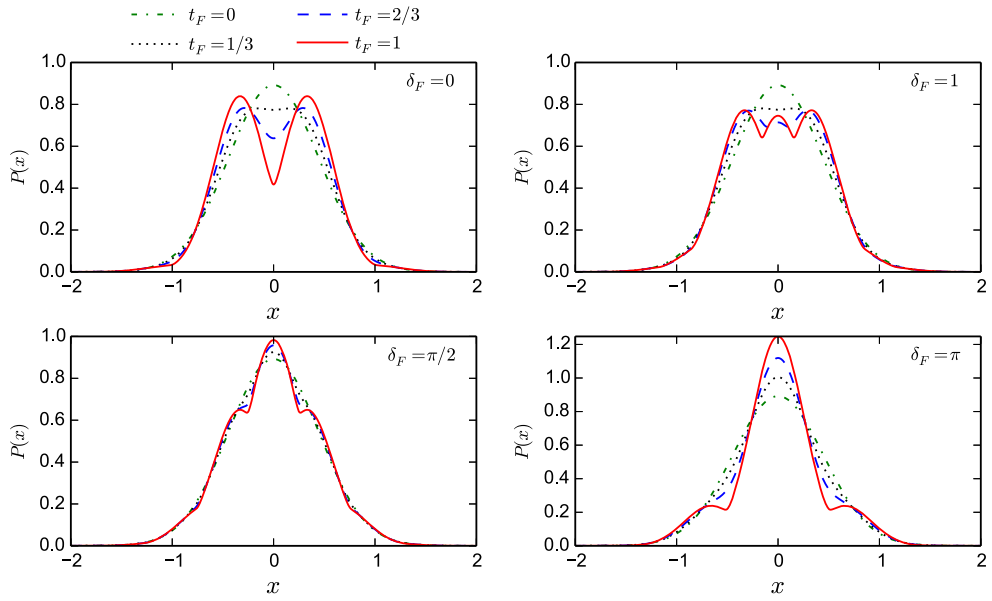

Fig. 2. The stationary probability distribution $P(x)$ of the dimensionless magnetic flux x in the classical Smoluchowski regime for the external magnetic flux $x_e = 0$ and four values of the phase δ_F of the transmission coefficient. In each panel there are four curves which correspond to different values of the amplitude of the transmission coefficient: $t_F = 0$ (green dashed–dotted), $1/3$ (black dotted), $2/3$ (blue dashed) and 1 (red solid). Other parameters are: $\alpha = 0.1$, $k_0 = 1$ and $T_0 = 0.2$. (For interpretation of the references to color in this figure legend, the reader is referred to the web version of this article.)

3.1. Stationary states

The stationary solution of the Fokker–Planck equations (13) and (23) is given by the steady-state probability distribution $P(x)$ through the relations (18) and (25) without and with the quantum corrections, respectively. We consider the case $x_e = 0$, i.e. when the external magnetic field is absent. In the case of classical thermal fluctuations, the Boltzmann distribution is depicted in Fig. 2 for four different values of the phase of the transmission coefficient $\delta_F = 0$ (top-left), 1 (bottom-left), $\pi/2$ (top-right), π (bottom-right). For $x_e = 0$, the probability distribution is symmetric with respect to the reflection $x \to -x$. Moreover, it is invariant under the change of the phase $P(x, \delta_F) = P(x, 2\pi - \delta_F)$. Therefore below we consider the interval of the phase $\delta_F \in [0, \pi]$. All four panels present the distributions for four different transmission coefficient $t_F = 0, 1/3, 2/3, 1$.

For full transmission (i.e. $t_F = 1$) the distribution possesses two local maxima for low valued phases, which reflects the bistability of the generalized thermodynamic potential Ψ_C. This, in turn, means that in the steady-state the current can flow in two directions: clockwise or counterclockwise (but the averaged current is zero!). For the phase $\delta_F \simeq 1$ and full transmission three local maxima can be found, with the most probable aside the local maximum around $x = 0$ (which denotes the zero current state). The additional local extrema, which doesn't appear in the $\delta_F \to 0$ case, indicate the possible multi-stability. This means that again the self-sustaining persistent currents can appear without the applied magnetic flux and are more probable than the zero current state. For the moderate-to-high phases the local maximum of the probability distribution at $x = 0$ becomes the most protruding among all others located at more distant values of the flux x. It means that self-sustaining currents are difficult to induce. Moreover, the lifetimes of the induced currents related to the remote from zero extrema are also expect to be relatively short [34].

As already stated, in the quantum Smoluchowski limit, the stationary solution (25) describes the thermodynamic equilibrium. It is not, however, the quantum Gibbs state, as we deal with the strong coupling to the environment. In this case, the probability distribution depends explicitly on the coupling of the ring with thermostat via the resistance R in the parameter λ_0 in Eq. (21). The equilibrium stationary distribution with quantum corrections is depicted in Fig. 3 for the same set of the parameters as in the classical counterpart in Fig. 2. For the quantum corrections we set $\lambda_0 = 0.001$ and $\epsilon = 100$. This means that the difference between the quantum and classical fluctuations of the dimensionless magnetic flux is $\lambda = 0.0075$. The corrected distribution display somehow magnified features seen in the corresponding classical cases: minima are deeper and maxima are more pronounced.

3.2. Current-flux characteristics

In previous papers [15,16], impact of quantumness of thermal fluctuations on the current-flux characteristics has been studied. In this section we will focus on influence of the quantum dot on such characteristics. For zero external magnetic flux, $x_e = 0$, the averaged stationary current is zero. It follows from the properties of the stationary distribution: it is an even function of x. The non-zero magnetic flux $x_e \neq 0$ breaks the x-reversal symmetry and the non-zero averaged current can emerge. In Fig. 4 we depict the response of the metallic ring to the applied constant magnetic flux in the classical Smoluchowski regime (i.e. for $\lambda = 0$). It is worth to stress that the current characteristics for the amplitude $t_F = 1$ and the phase $\delta_F = 0$ of the transmission coefficient (top panel, red curve) represent the situation with maximal current. In other words, it is the same as the ring without quantum dot. The suppression of the generated signal which comes with the reduction of the transmission amplitude seems to be the usual situation. For $t_F = 0$ it is impossible to generate current in the ring. For the phase $\delta_F \in (-\pi/2, \pi/2)$ the current response of the ring is paramagnetic for all non-zero amplitudes t_F. In turn, for $\delta_F \in (\pi/2, 3\pi/2)$ the response is diamagnetic. Let us note the doubled period for the particular case $\delta_F = \pi/2$. The analysis for slightly lower or higher phases shows simple para- or diamagnetic single-periodic structure of current-flux characteristics, respectively.

We now address the issue of whether, and to which extent, the quantum nature of thermal fluctuations can influence transport properties. We thus show impact of quantum corrections on the current characteristics in Fig. 5 for the fixed quantumness parameters $\lambda_0 = 0.001$ and $\epsilon = 100$. This figure is organized in exactly

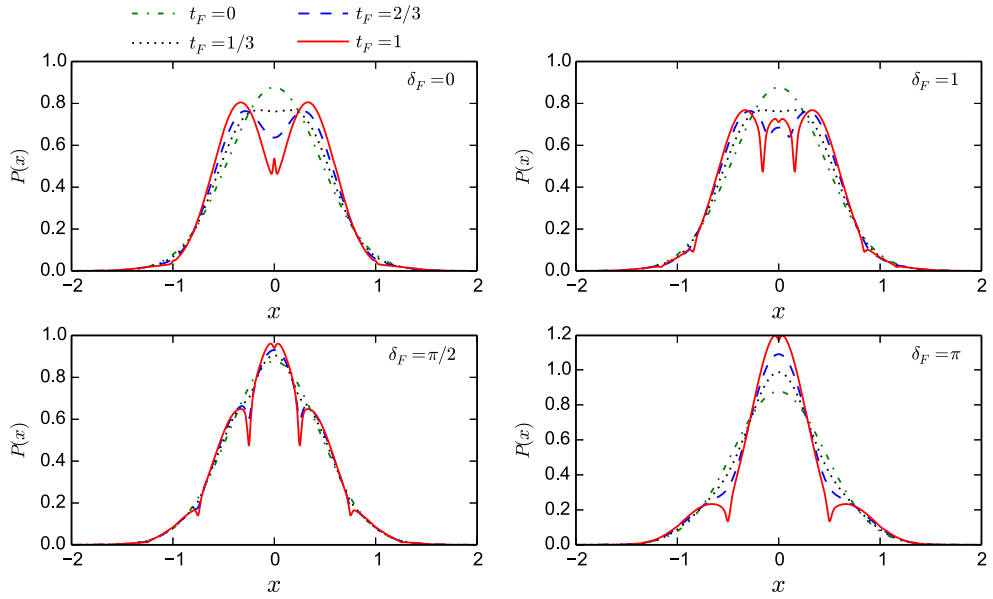

Fig. 3. The stationary probability distribution $P(x)$ in the quantum Smoluchowski regime for $x_e = 0$ and four values of the phase δ_F of the transmission coefficient. In each panel there are four curves which correspond to selected values of the amplitude of the transmission coefficient: $t_F = 0$ (green dashed–dotted), 1/3 (black dotted), 2/3 (blue dashed) and 1 (red solid). The remaining parameters read $\alpha = 0.1$, $k_0 = 1$, $T_0 = 0.2$, $\lambda_0 = 0.001$ and $\epsilon = 100$. (For interpretation of the references to color in this figure legend, the reader is referred to the web version of this article.)

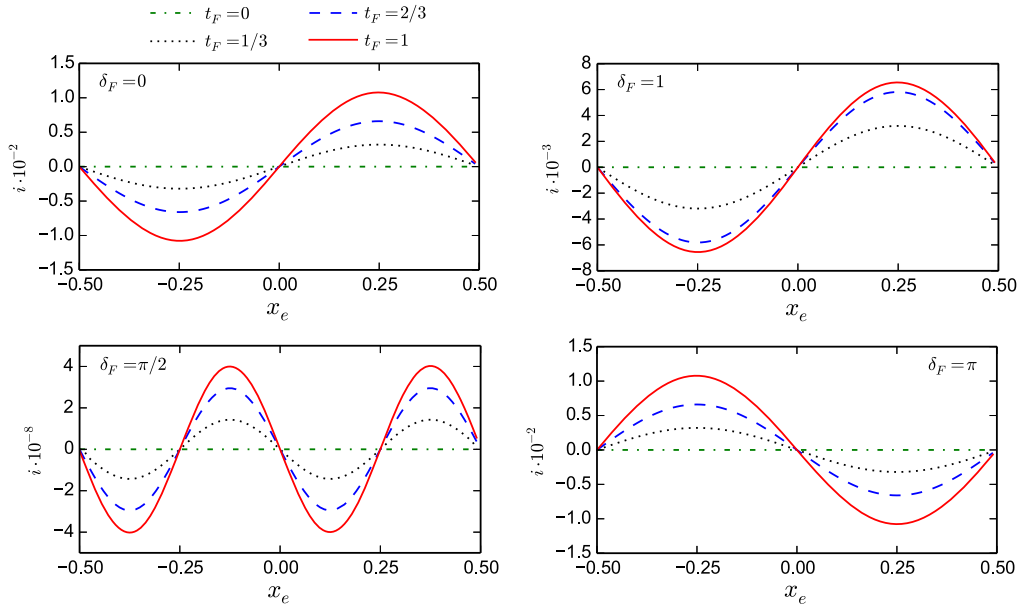

Fig. 4. The stationary averaged current i in the classical Smoluchowski regime versus the external magnetic flux x_e is presented for four different values of the phase δ_F. In each panel there are four curves which correspond to selected values of the amplitude of the transmission coefficient: $t_F = 0$ (green dashed–dotted), 1/3 (black dotted), 2/3 (blue dashed) and 1 (red solid). Other system parameters read $\alpha = 0.1$, $k_0 = 1$, $T_0 = 0.2$. (For interpretation of the references to color in this figure legend, the reader is referred to the web version of this article.)

the same way as the previous one although the peculiarities are slightly different. For instance we cannot conclude here, that the maximal possible current amplitude is typically realized for $t_F = 1$. In the classical Smoluchowski regime, the case $t_F = 1$ is always the most optimal. With quantum corrections, it is intriguing to note that around $\delta_F = \pi/2$ the maximal amplitude of the transmission coefficient does not provide maximal current. In fact the current is weaker for $t_F = 1$ than for $t_F = 2/3$ or even when $t_F = 1/3$, see Fig. 5. In fact one can observe something similar to the transition from the paramagnetic to the diamagnetic state simply by changing the phase around $\delta_F = \pi/2$. This is displayed in Fig. 6. For the phases a little bit higher than $\pi/2$, like one identify the classical picture – c.f. bottom panel in Fig. 5.

As the next point of analysis we ask about domains of parameters δ_F and t_F where the current is paramagnetic and diamagnetic, see Fig. 6. In the case of classical thermal fluctuations, the current is always of a paramagnetic type in the interval $\delta_F \in (0, \pi/2) \cup (3\pi/2, 2\pi)$ and is always of a diamagnetic type for $\delta_F \in (\pi/2, 3\pi/2)$. In the case of quantum thermal fluctuations, it is not true: these intervals depend on the amplitude of the transmission coefficient. Nevertheless, the current is paramagnetic in a large interval around $\delta_F = 0$ and is diamagnetic in a large interval around $\delta_F = \pi$, and the transition point is in a small interval around $\delta_F = \pi/2$. The type of response is more robust to changes in the amplitude of the transmission coefficient and more sensitive to changes of the phase around the value $\pi/2$.

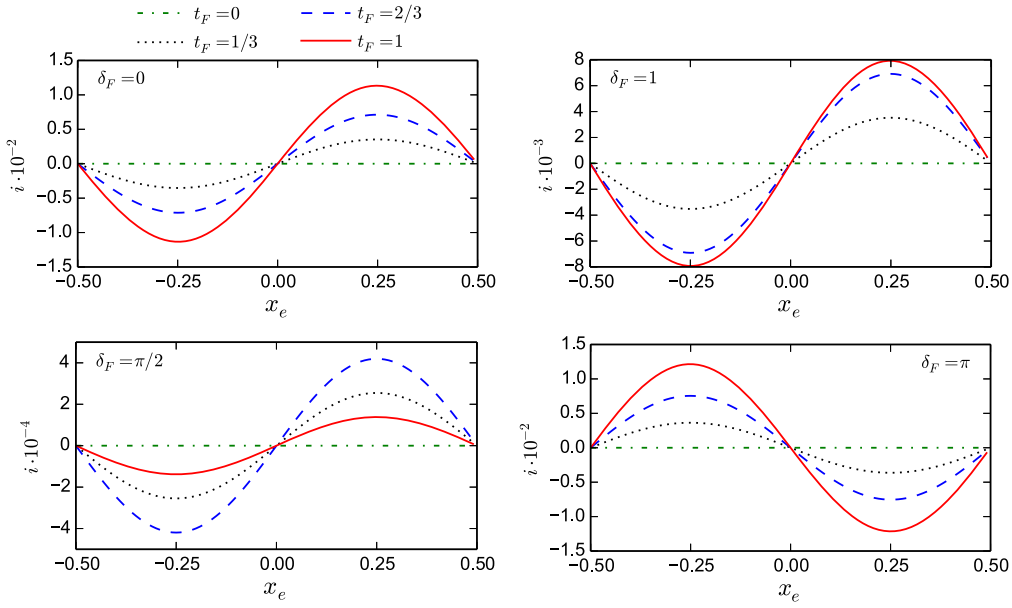

Fig. 5. The stationary averaged current i in the quantum Smoluchowski regime versus the external magnetic flux x_e is presented for four values of the phase δ_F and four values of the amplitude of the transmission coefficient: $t_F=0$ (green dashed–dotted), 1/3 (black dotted), 2/3 (blue dashed) and 1 (red solid). Other system parameters read $\alpha=0.1$, $k_0=1$, $T_0=0.2$, $\lambda_0=0.001$ and $\epsilon=100$. (For interpretation of the references to color in this figure legend, the reader is referred to the web version of this article.)

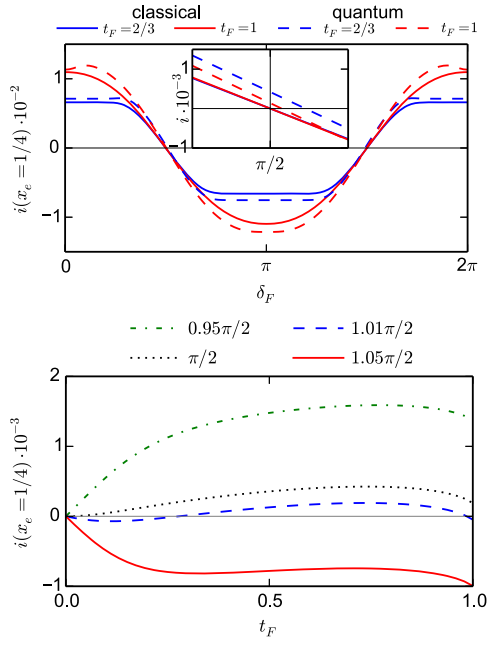

Fig. 6. The regimes of paramagnetic ($i>0$) and diamagnetic ($i<0$) response in dependence of the phase δ_F and the amplitude t_F of the transmission coefficient through a quantum dot for an electron of the Fermi energy. The external magnetic flux is fixed at $x_e=1/4$. For the phase close to $\pi/2$ the current reversal is observed (upper panel). In bottom panel, the stationary averaged current in the quantum Smoluchowski regime is depicted as a function of the amplitude t_F and in the vicinity of the phase $\delta_F=\pi/2$. Four curves correspond to four values of the phase $\delta_F=0.95\pi/2, \pi/2, 1.01\pi/2, 1.05\pi/2$. Other system parameters read $\alpha=0.1$, $k_0=1$, $T_0=0.2$, $\lambda_0=0.001$ and $\epsilon=100$.

4. Summary

This paper presents the influence of the quantum dot on transport properties of mesoscopic non-superconducting rings. The theory is constructed in the framework of the Langevin equation for overdamped dynamics of the magnetic flux. We have considered the case when the system is driven by classical thermal noise in the Smoluchowski regime. It was then extended to account for quantum effects within the quantum Smoluchowski equation. The stationary probability distribution both in 'classical' and 'quantum' case is depicted for zero external magnetic flux. The current-flux characteristics are analyzed in detail. The impact of parameters characterizing the quantum dot on the current has been addressed in this work. The phase of the transmission coefficient plays the crucial role. In the 'classical' case, its crossover value is fixed to $\delta_F=\pi/2$. Below this value, the current is paramagnetic while above this value the current is diamagnetic. For the 'quantum' case, the response threshold depends on other parameters of the system, nevertheless it is located close to the value $\pi/2$. Finally, we would like to mention that recent progress in entirely novel experimental techniques makes the verification of our findings possible and we hope that our work will contribute to the development of effective control methods of transport properties in mesoscopic systems.

Acknowledgement

The work supported in part by the NCN grant DEC-2013/09/B/ST3/01659.

References

[1] L.P. Lévy, G. Dolan, J. Dunsmuir, H. Bouchiat, Phys. Rev. Lett. 64 (1990) 2074.
[2] V. Chandrasekhar, R.A. Webb, M.J. Brady, M.B. Ketchen, W.J. Gallagher, A. Kleinsasser, Phys. Rev. Lett. 67 (1991) 3578.
[3] D. Mailly, C. Chapelier, A. Benoit, Phys. Rev. Lett. 70 (1993) 2020.
[4] F. Hund, Ann. Phys. 32 (1938) 102;
F. Hund, Ann. Phys. 5 (1996) 1.
[5] Y. Imry, Introduction to Mesoscopic Physics, Oxford University Press, 1997.
[6] F. Bloch, Phys. Rev. 137 (1965) 787.
[7] I.O. Kulik, JETP Lett. 11 (1970) 275.
[8] M. Büttiker, Y. Imry, R. Landauer, Phys. Lett. A 96 (1983) 365.
[9] E.M.Q. Jariwala, P. Mohanty, M.B. Ketchen, R.A. Webb, Phys. Rev. Lett. 86 (2001) 1594.
[10] W. Rabaud, L. Saminadayar, D. Mailly, K. Hasselbach, A. Benoît, B. Etienne, Phys. Rev. Lett. 86 (2001) 3124.
[11] H. Bluhm, N.C. Koshnick, J.A. Bert, M.E. Huber, K.A. Moler, Phys. Rev. Lett. 102 (2009) 136802.
[12] Y. Imry, Physics 2 (2009) 24.
[13] A.C. Bleszynski-Jayich, W.E. Shanks, B. Peaudecerf, E. Ginossar, F. von Oppen, L. Glazman, J.G.E. Harris, Science 326 (2009) 272.
[14] J. Dajka, J. Łuczka, M. Szopa, E. Zipper, Phys. Rev. B 67 (2003) 073305.

[15] L. Machura, Sz. Rogoziński, J. Łuczka, J. Phys. Condens. Matter 22 (2010) 422201.
[16] Sz. Rogoziński, L. Machura, J. Łuczka, Eur. Phys. J. Spec. Top. 187 (2010) 5.
[17] A. Yacoby, M. Heiblum, D. Mahalu, H. Shtrikmann, Phys. Rev. Lett. 74 (1995) 4047.
[18] A. Levy Yeyati, M. Büttiker, Phys. Rev. B 52 (1995) R14360.
[19] G. Hackenbroich, H.A. Weidenmüller, Phys. Rev. B 53 (1996) 16379.
[20] J. Wu, B.-L. Gu, H. Chen, W. Duan, Y. Kawazoe, Phys. Rev. Lett. 80 (1998) 1952.
[21] I. Affleck, P. Simon, Phys. Rev. Lett. 86 (2001) 2854.
[22] K. Bao, Y. Zheng, Phys. Rev. B 73 (2005) 045306.
[23] H.-P. Eckle, H. Johannesson, C.A. Stafford, Phys. Rev. Lett. 87 (2001) 016602.
[24] S.Y. Cho, K. Kang, C.K. Kim, C.-M. Ryu, Phys. Rev. B 64 (2001) 033314.
[25] G.-H. Ding, B. Dong, Phys. Rev. B 67 (2003) 195327.
[26] C. Somaschini, S. Bietti, N. Koguchi, S. Sanguinetti, Nanotechnology 22 (2011) 185602.
[27] S. Sanguinetti, C. Somaschini, S. Bietti, N. Koguchi, Nanomater. Nanotechnol. 1 (2011) 14.
[28] E. Zipper, M. Kurpas, M.M. Maska, New J. Phys. 14 (2012) 093029.
[29] M.V. Moskalets, Europhys. Lett. 39 (1997) 425.
[30] H.F. Cheung, Y. Gefen, E.K. Riedel, W.H. Shih, Phys. Rev. B 37 (1989) 6050.
[31] R. Kubo, Rep. Prog. Phys. 29 (1966) 255.
[32] R. Zwanzig, J. Stat. Phys. 9 (1973) 215.
[33] J. Dajka, S. Rogoziński, L. Machura, J. Łuczka, Acta Phys. Pol. B 38 (2007) 1737.
[34] J. Dajka, L. Machura, S. Rogoziński, J. Łuczka, Phys. Rev. B 76 (2007) 045337.
[35] C.W. Gardiner, Handbook of Stochastic Methods, Springer, Berlin, 1983.
[36] J. Ankerhold, P. Pechukas, H. Grabert, Phys. Rev. Lett. 87 (2001) 086802.
[37] L. Machura, M. Kostur, P. Hänggi, P. Talkner, J. Łuczka, Phys. Rev. E 70 (2004) 031107.
[38] J. Łuczka, R. Rudnicki, P. Hänggi, Physica A 351 (2005) 60.
[39] L. Machura, M. Kostur, P. Talkner, J. Łuczka, P. Hänggi, Phys. Rev. E 73 (2006) 031105.
[40] L. Machura, J. Łuczka, P. Talkner, P. Hänggi, Acta Phys. Pol. B 38 (2007) 1855.
[41] W.T. Coffey, Y.P. Kalmykov, S.V. Titov, L. Cleary, Phys. Rev. E 78 (2008) 031114.
[42] L. Cleary, W.T. Coffey, Y.P. Kalmykov, S.V. Titov, Phys. Rev. E 80 (2008) 051106.
[43] W.T. Coffey, Y.P. Kalmykov, S.V. Titov, L. Cleary, Phys. Rev. B 79 (2009) 054507.
[44] S. Maier, J. Ankerhold, Phys. Rev. E 81 (2010) 021107.